ISSN 1674-1056
http://cpb.iphy.ac.cn
http://iopscience.iop.org/cpb
中国物理 B
Chinese Physics
中国物理
Chinese Physics B

Adsorption and desorption phenomena on thermally annealedmulti-walled carbon nanotubes by XANES study

Camile Rodolphe Tchenguem Kamto, Bridinette Thiodjio Sendja, Jeannot Mane Mane

Citation: Chin. Phys. B . 2019, 28(9): 093101 . **doi:** 10.1088/1674-1056/28/093101
Journal homepage: http://cpb.iphy.ac.cn; http://iopscience.iop.org/cpb

What follows is a list of articles you may be interested in

Landscape of s-triazine molecule on Si(100) by a theoretical x-ray photoelectron spectroscopy and x-ray absorption near-edge structure spectra study

Jing Hu(胡静), Xiu-Neng Song(宋秀能), Sheng-Yu Wang(王胜雨), Juan Lin(林娟), Jun-Rong Zhang(张俊荣), Yong Ma(马勇)

Chin. Phys. B . 2018, 27(11): 113101 . **doi:** 10.1088/1674-1056/27/11/113101

Determination of static dipole polarizabilities of Yb atom

Zhi-Ming Tang(唐志明), Yan-Mei Yu(于艳梅), Chen-Zhong Dong(董晨钟)

Chin. Phys. B . 2018, 27(6): 063101 . **doi:** 10.1088/1674-1056/27/6/063101

Selection rules for electric multipole transition of triatomic molecule in scattering experiments

Hong-Chun Tian(田红春), Long-Quan Xu(徐龙泉), Lin-Fan Zhu(朱林繁)

Chin. Phys. B . 2018, 27(4): 043101 . **doi:** 10.1088/1674-1056/27/4/043101

Na decorated B_6 cluster and its hydrogen storage properties

Ruan Wen, Wu Dong-Lan, Luo Wen-Lang, Yu Xiao-Guang, Xie An-Dong

Chin. Phys. B . 2014, 23(2): 023102 . **doi:** 10.1088/1674-1056/23/2/023102

Density functional theory study of the interaction of H_2 with pure and Ti-doped WO_3 (002) surfaces

Hu Ming,Wang Wei-Dan,Zeng Peng,Zeng Jing,Qin Yu-Xiang

Chin. Phys. B . 2012, 21(2): 023101 . **doi:** 10.1088/1674-1056/21/2/023101

Adsorption and desorption phenomena on thermally annealed multi-walled carbon nanotubes by XANES study

Camile Rodolphe Tchenguem Kamto[1], Bridinette Thiodjio Sendja[2,†], and Jeannot Mane Mane[2,3]

[1] University of Yaounde I, Faculty of Science, Department of Physics, Yaounde, Cameroon
[2] University of Yaounde I, National Advanced School of Engineering, Department of Mathematic and Physical Science, Yaounde, Cameroon
[3] University of Dschang, Dschang, Cameroon

(Received 15 May 2019; revised manuscript received 12 July 2019; published online 30 August 2019)

The multi-walled carbon nanotubes (MWCNTs) studied in this work were synthesized by the catalytic chemical vapor deposition (CCVD) process, and were thermally annealed by the hot filament plasma enhanced (HF PE) method at 550 °C for two hours. The x-ray absorption near edge structure (XANES) technique was used to investigate the adsorption and desorption phenomena of the MWCNTs at normal and grazing incidence angles. The adsorbates were found to have different sensitivities to the thermal annealing. The geometry of the incident beam consistently gave information about the adsorption and desorption phenomena. In addition, the adsorption of non-intrinsic potassium quantitatively affected the intrinsic adsorbates and contributed to increase the conductivity of the MWCNTs. The desorption of potassium was almost 70% greater after the thermal annealing. The potassium non-intrinsic adsorbates are from a physisorption mechanism whereas the intrinsic adsorbates result from chemisorption.

Keywords: multi-walled carbon nanotubes, thermal annealing, adsorption, desorption

PACS: 31.10.+z, 31.15.ae, 32.30.Rj, 82.80.Dx **DOI:** 10.1088/1674-1056/ab3437

1. Introduction

The theoretical and experimental knowledge of the structure of a system is required to elucidate new materials with novel properties. Carbon nanotubes (CNTs) have intensively undergone theoretical and experimental studies because of their versatilities. During the first decade of the discovery of CNTs by Sumio Iijima, they were usually obtained at high temperature (about 3500 ℃) using graphite electrodes by the electric discharge process.[1] Nowadays, they are produced in industries at intermediate temperatures (between 700–950 ℃) by the well-known catalytic chemical vapor deposition (CCVD) process,[2,3] electric discharge,[1] or laser ablation.[4] Among these, CCVD is one of the most suitable methods for synthesizing aligned CNTs since it can be carried out at low temperatures and pressures.[5] However, CCVD synthesized CNTs usually contain catalytic metallics and impurities whose nature and proportion depend on the synthesis parameters. The presence of impurities can significantly affect the properties of CNTs and consequently the global behavior of these materials.[6] The samples studied herein are multi-walled CNTs (MWCNTs) synthesized by the hot filament plasma enhanced catalytic chemical vapor deposition (HF PE CCVD) process fully described in Ref. [7]. CNTs are mostly characterized by scanning electron microscopy (SEM)[8] and transmission electron microscopy (TEM),[9] which are both qualitative methods. These techniques do not give enough information about the electronic and structural properties of the CNTs. The x-ray absorption near edge structure (XANES) technique on the contrary is a powerful tool that provides the structural and electronic information on the local environment around the absorber atom in the medium range order due to its angular dependence of the absorption transition.[7] This technique is sensitive to the chemical adsorption and impurities, defects, and orbital rehybridization.[7] MWCNTs with large diameter are advantageous for various applications like molecular compounds for instance, in organic solar cells,[10] infrared detectors,[11] and biological systems.[12] The adsorption and desorption phenomena of the MWCNTs are of great interest since they provide a full understanding of the performance for water and wastewater treatment applications.

In this study, through XANES technique, we investigate the adsorption and desorption phenomena of MWCNTs grown by CCVD process and thermally annealed at 550 ℃. The XANES spectra are collected at normal incidence (NI) and grazing incidence (GI) angles to evaluate the adsorption percentage.

2. Theory

MWCNT is made up of a bundle of single walled CNTs (SWCNT) arranged such that they all have the same vertical axis. The external diameter of the MWCNT depends on the growth process. By the electric arc discharge, the external diameter is about 20 nm, whereas it can reach 100 nm with the CCVD process.[2] In general, as a consequence of the synthesis process, the surfaces of the CNTs are usually covered by some adsorbates mostly considered as impurities.[13] These

†Corresponding author. E-mail: sbridine@yahoo.fr

© 2019 Chinese Physical Society and IOP Publishing Ltd

adsorbates can affect, in different ways, the structure of the surfaces since they can be linked physically by van der Waals forces or chemical covalent bonds.[13] The former is named physisorption mechanism while the latter is chemisorption. If the free bonds are saturated, the strongly linked adsorbates can either eliminate or favor the restructuring of the free surface, which thus may or may not affect the properties of the surface.[13] It has been established that the Lennard–Jones interactions prevail in the adsorption mechanism,[14] suggesting that the interaction potential V between two species with a distance r can be written as a sum of the terms of the repulsion and attraction contributions, as follows:

$$V = \varepsilon \left[\left(\frac{r_0}{r} \right)^{12} - 2 \left(\frac{r_0}{r} \right)^{6} \right], \tag{1}$$

where ε and r_0 are the Lennard–Jones parameters for each couple of species at the equilibrium distance.

Chemisorption is a dominant process in SWCNTs.[15] On the contrary, physisorption, which is a characteristic of MWCNTs, is a reversible process that can occur at low temperatures.[15] Adsorption capacity depends on the specific surface area and the number of walls in the MWCNT. The specific surface area reduces with an increase in diameter and in the number of walls.[16] The average specific surface area of the MWCNTs is between 30 m^2/g and 400 m^2/g depending on the mean diameter and the number of walls.[16] The specific surface area S of a MWCNT is given by[16]

$$S = \frac{2}{\rho(R_1 - R_2)} = \frac{2630}{n} \quad [m^2/g], \tag{2}$$

where R_1 and R_2 are the external and internal radii, respectively, and n is the number of walls. In the above formula, the density $\rho = 2.26$ g/cm^3 and $R_1 - R_2$ is 3.36 Å, which correspond to those of graphite. Physisorption offers the possibility to modify the electronic properties of the substrate. The adsorbate species can leave the surface, leading to desorption, their speciation and the determination of their characteristics can allow to extract valuable information on the desorption process. This can be done by breaking the chemical or physical bonds existing on the surface. XANES spectroscopy is a powerful tool that can give structural and electronic information on the atoms and molecules as well as the local chemical functionalities.[17] The experimental details and the CCVD growth process of our studied MWCNTs have been fully described elsewhere.[7,18]

3. Results and discussion

The XANES spectra collected at the carbon K edge are shown in Figs. 1 and 2. The data have been collected at normal incidence angle ($\theta = 0°$ with $\boldsymbol{E}$ parallel to the surface) (Figs. 1(a) and 2(a)) and at grazing incidence angle ($\theta = 90°$ with $\boldsymbol{E}$ normal to the surface) (Figs. 1(b) and 2(b)). Note that θ is the angle between the axis of the sample and the direction of the electric field vector $\boldsymbol{E}$ of the x-ray incident beam. The XANES spectra can be divided into three main regions as described in Ref. [18]. The first region located at 285.5 eV corresponds to peak A. The second region between 286.5 eV and 290.5 eV is assigned to the free electron like interlayer (FELI) states and the adsorbed or chemisorbed molecular states. The third region, corresponding to the transitions towards the σ^* and π^* empty states is above 291.8 eV. From our XANES spectra, the intrinsic and non-intrinsic adsorbates can be distinguished. The intrinsic adsorbates, namely, A′, A″, A‴, and A⁗ are the results of the gas, atomic, and/or molecular adsorption of different species such as oxygen (O_2), water (H_2O), and transition metals (TM) during the synthesis process.[7,19] The non-intrinsic adsorbate observed in our XANES spectra (Fig. 2) is attributed to the potassium element which appears accidentally during the synthesis process.[18]

Tables 1 and 2 show the intrinsic and non-intrinsic adsorbates with their corresponding intensities and final states in the Brilouin zone, for annealed and un-annealed samples contaminated with potassium, respectively.

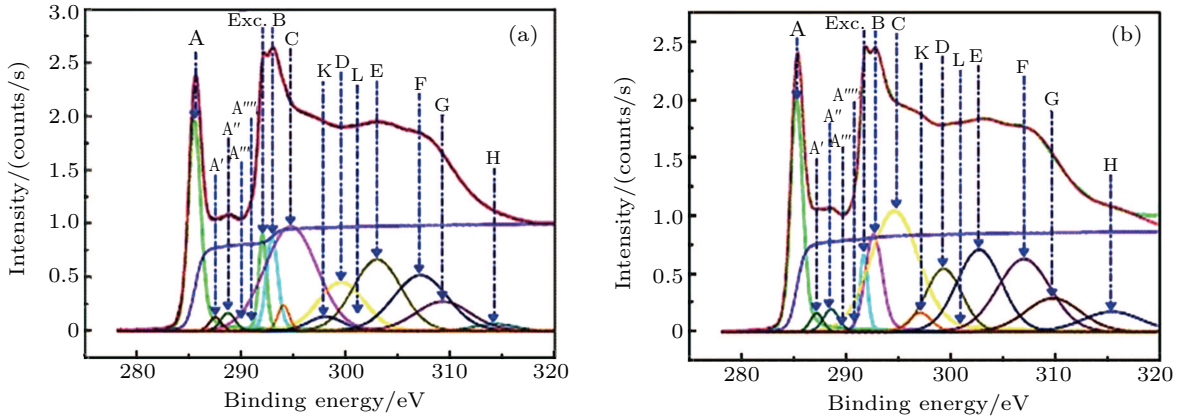


Fig. 1. Experimental and simulated XANES spectra of MWCNTs annealed and without contaminants at (a) normal and (b) grazing incidences.

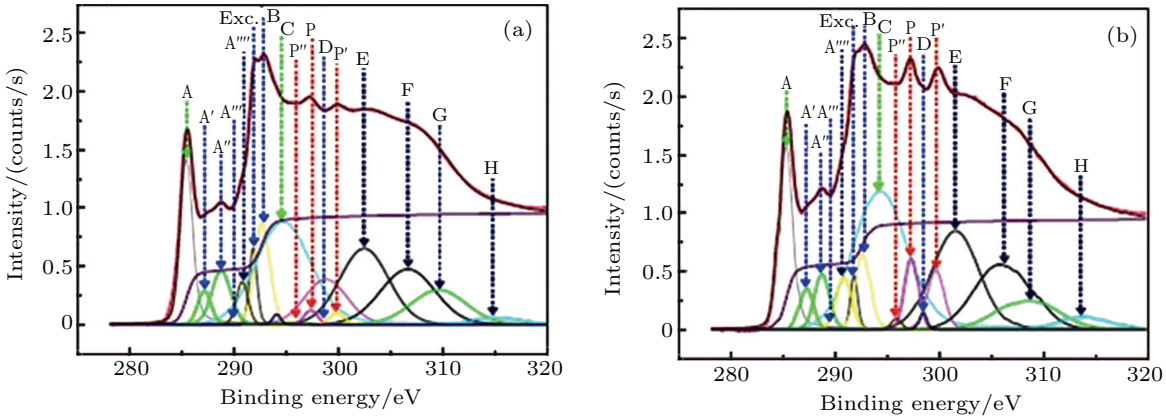


Fig. 2. Experimental and simulated XANES spectra of MWCNTs annealed and contaminated with potassium at (a) normal and (b) grazing incidences.

Table 1. Main feature parameters for annealed and potassium-contaminated MWCNTs from XANES spectra at normal and grazing incidence angles. The intensity is in units of counts per second.

Adsorbates	Energy/eV	Intensity at NI	Intensity at GI	Final-state band and Brillouin-zone
A′	286.53	0.46	0.46	free-electron-like interlayer states + adsorption
A″	288.40	1.10	1.02	free-electron-like interlayer states + adsorption
A‴	288.70	0.0	0.0	free-electron-like interlayer states + adsorption
A⁗	290.70	0.52	0.63	free-electron-like interlayer states + adsorption
P″	297.51	0.0	0.0	potassium L_2 level
P	296.60	0.19	0.17	potassium L_2, L_3 level
P′	299.83	0.17	0.20	potassium L_2–L_1 levels

Table 2. Main feature parameters for unannealed and potassium-contaminated MWCNTs from XANES spectra at grazing and normal incidence angles. The intensity is in units of counts per second.

Adsorbates	Energy/eV	Intensity at NI	Intensity at GI	Final-state band and Brillouin-zone
A′	286.53	0.67	0.86	free-electron-like interlayer states + adsorption
A″	288.40	1.57	1.90	free-electron-like interlayer states + adsorption
A‴	288.70	0.0	0.29	free-electron-like interlayer states + adsorption
A⁗	290.70	0.85	1.10	free-electron-like interlayer states + adsorption
P″	297.51	0.03	0.03	potassium L_2 level
P	296.60	1.02	1.39	potassium L_2, L_3 level
P′	299.83	1.39	1.55	potassium L_2–L_1 levels

Each adsorbate corresponds to a specific electronic transition which is assigned to peaks A′, A″, A‴, and A⁗ or P, P′, and P″. These peaks are strongly linked to the height of the adsorbates. Also, the probability for a chemical species to be adsorbed depends on the nature of the surface. The types of bonds and the associated physical properties considerably depend on the types of the adsorbed atoms.[22] The quantity of the adsorbates on the surface varies as a function of the curvature radius of the CNTs since the adsorption strongly depends on the specific surface area.[19]

The individual contributions of the adsorbates present in our samples exhibit significant differences at normal and grazing incidence angles. During the adsorption process, rehybridization can occur in which the sp^2 and sp^3 orbitals are mixed leading to two free hybrid orbitals. Such that, if the contribution of sp^3 increases, this will lead to the presence of more free bonds, resulting in the increase of the reactivity.

Figure 3 presents a comparison of the histogram of the intensities of the contaminated MWCNTs un-annealed and annealed for different adsorbates at normal and grazing incidence angles respectively.

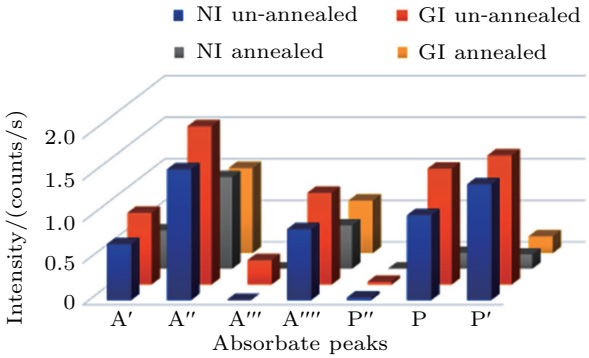


Fig. 3. The trend of the intensities of the adsorbates for the contaminated un-annealed and annealed MWCNTs at normal and grazing incidence angles.

Comparing the intensities of the annealed and un-annealed contaminated MWCNTs shows that the non-intrinsic

adsorbates A′ and A‴ almost disappear in the presence of potassium adsorbates in the two studied angles. The quantity of the intrinsic adsorbates considerably reduces after the thermal annealing process at normal and grazing incidences. It can also be seen that the non-intrinsic adsorbates are less sensitive to the thermal treatment. However, it is shown that when the potassium is adsorbed at 12%, the intrinsic adsorbates increase by 2.12 and 1.64 times at normal and grazing incidence angles, respectively. At normal incidence, the x-ray beam is parallel to the surface of the sample, hence the π states are excited to π^* and some adsorbed chemical species are masked by others. On the contrary, at grazing incidence where the x-ray beam is perpendicular to the surface, the σ states are excited to σ^*. These findings show that the adsorption process is also affected by the direction of the x-ray beam as demonstrated by Huang *et al.*[6] It can be understood that the adsorbates are either affected or desorbed with different sensitivities. This can be explained by the types of bonds that are formed on the surface and/or the temperature of the annealing process (which might not be sufficient). Quantification of the sensitivity of the adsorbates can provide information on the purification method. Thus, the desorption yield of the adsorbates can be expressed as

$$Rdt = \frac{I_{\text{initial}} - I_{\text{final}}}{I_{\text{initial}}} \times 100\%, \tag{3}$$

where I_{initial} and I_{final} are the intensities of the adsorbates before and after thermal annealing, respectively. The histogram representing the desorption yield of the adsorbates evaluated from XANES results is shown in Fig. 4 at normal incidence and grazing incidence angles.

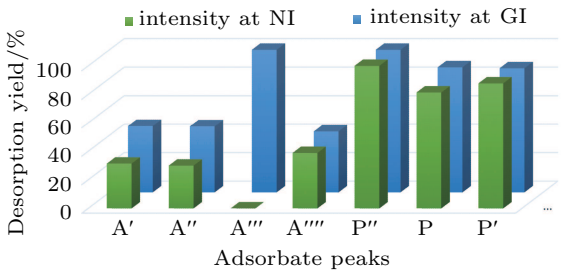


Fig. 4. Desorption yield of the adsorbates at normal incidence and grazing incidence angles.

It can be observed that potassium adsorbates (P, P′, and P″) are more sensitive to thermal annealing compared to the intrinsic adsorbates (A′, A″, A‴, and A⁗). Also, the geometry at grazing incidence angle is favorable to the desorption process. On the one hand, the high sensitivity of potassium adsorbates to the thermal annealing demonstrates that the physical bonds are established on the surface, leading to the physisorption mechanism. On the other hand, since the intrinsic adsorbates are not sensitive enough to the thermal annealing, suggesting the existence of chemical bonds on the surface, the chemisorption mechanism can be attributed to these types of adsorbates. Chemical bonds are more difficult to break. Incidentally, the potassium donor species can easily be used to dope the MWCNTs. Ding *et al.*[23] and Dresselhaus *et al.*[24] showed that doping the SWCNTs with potassium can improve the conductivity and Fermi energy. The conductivity of our MWCNT is modified in the presence of potassium and is increased by about 12% after thermal annealing.

4. Conclusion

The characterization of the carbon nanostructures after synthesis is mandatory since the properties of these materials can be well understood for applications related to adsorption and desorption. These nanostructures can then be applied to solve problems of water, air, and soil purification. XANES spectroscopy was used to qualitatively and quantitatively evaluate the adsorbed species on the MWCNTs. We observed that the quantity adsorbed on the surface is proportional to the diameter of the multi-walls. In addition, the incident angle of the incoming beam plays a key role in understanding the adsorption phenomenon. The results showed that the potassium non-intrinsic adsorbates are resulted from the physisorption mechanism whereas the intrinsic adsorbates are from chemisorption. Also, the intrinsic adsorbates are less sensitive to the thermal treatment compared to the non-intrinsic potassium adsorbates. In addition, it is seen that the presence of potassium increases the conductivity of the MWCNTs after thermal treatment, and the desorption process is mostly affected at grazing incidence. It is worth noting that the adsorbates are useful for non-covalent functionalization with potential applications in electronic, biologic, water treatment, and environmental protection. Moreover, thermal annealing is one of the efficient methods for the purification and controlling the conductivity of the MWCNTs.

Acknowledgment

P. Legagneux, Accosta, G. Schmerber, and F Le Normand are acknowledged for providing experimental data.

References

[1] Iijima S 1991 *Nature* **354** 56
[2] Dresselhaus M S, Dresselhaus G and Avouris P 2001 *Carbon Nanotubes: Synthesis, Structure, Properties And Applications* (Berlin: Springer) p. 29
[3] Cojocaru C S 2003 (Ph. D Thesis) (Université Louis Pasteur, Strasbourg I)
[4] Thess A, Lee R, Nikolaev P, Dai H, Petit P, Robert J, Xu C, Lee Y H, Kim S G, Rinzler A G, Colbert D T, Scuseria G E, Tomanek D, Fischer J E and Smalley R E 1996 *Science* **273** 483
[5] Lin K S, Mai Y J, Li S R, Shu C W and Wang C H 2012 *J. Nanomater* 939683
[6] Huang W, Wang Y, Luo G and Wie F 2003 *Carbon* **41** 2585
[7] Eba Medjo R, Thiodjio Sendja B, Mane Mane J and Owono Ateba P 2009 *Phys. Scr.* **80** 045601
[8] Cojocaru C S and Le Normand F 2006 *Thin Solid Films* **515** 53
[9] Taschner C, Pacal F, Leonhardt A, Spatenka P, Bartsch K, Graff A and Kaltofen R 2003 *Surf. Coat. Technol.* **174–175** 81

[10] Hatton R A, Blanchard N P, Miller A J and Silva S R P 2007 *Physica E* **37** 124

[11] Varghese O K, Kichambre P D, Gong D, Ong K G, Dickey E C and Grimes G A 2001 *Sens. Actuators B Chem.* **81** 32

[12] Zhu L, Chang D W, Dai L and Hong Y 2007 *Nano Lett.* **7** 3592

[13] Ibach H 2006 *Physics of Surfaces and Interfaces* (Berlin: Springer-Verlag) p. 30

[14] Lennard-Jones J E 1932 *Trans. Faraday Soc.* **28** 333

[15] Dabrowski A 2001 *Adv. Colloid Interface Sci.* **93** 135

[16] Peigney A, Laurent C, Flahaut E, Bacsa R R and Rousset A 2001 *Carbon* **39** 507

[17] Kuznetsova A, Popova I, Yates J T, Bronikowski M J, Huffman C B, Liu J, Smalley R E, Hwu H H and Chen J G 2001 *J. Am. Chem. Soc.* **123** 10699

[18] Eba Medjo R, Thiodjio Sendja B and Mane Mane J 2014 *Mater. Sci. Appl.* **5** 95

[19] Jun Z and Chang L 2005 *Xanes Study of Carbon Based Nanotubes* **29** *Conference proceedings*

[20] Eba Medjo R 2015 *Contamination in Manufacturing of Carbon Nanostructures*

[21] Rosenberg R A, Love P J and Rehn V 1986 *Phys. Rev. B* **33** 4034

[22] Durgun E, Dag S, Bagci V M K, *et al.* 2003 *Phys. Rev. B* **67** 201401(R)

[23] Ding Y, Yang X B and Ni J 2006 *Front. Phys. Chin.* **1** 317

[24] Dresselhaus M S, Williams K A and Eklund P C 1999 *MRS Bull.* **24** 45